

## Supporting Information

### **A General “Gas-Liquid” Synthesis Strategy Towards Centimeter-Scale Two-Dimensional Non-Layered Semiconductors**

Jiahui Liu<sup>‡,a</sup>, Jiangbo Yuan<sup>‡,a</sup>, Hao Liu<sup>‡,a</sup>, Zhiyi Yuan<sup>a</sup>, Baochuan Guo<sup>a</sup>, Shaohui Li<sup>a</sup>, Qihong Cui<sup>b,\*</sup>, Qun Xu<sup>a,\*</sup> and Cong Wei<sup>a,\*</sup>

<sup>a</sup> College of Materials Science and Engineering, Zhengzhou University, Zhengzhou 450001, China.

<sup>b</sup> Key Laboratory of Luminescence and Optical Information, Ministry of Education, Beijing Jiaotong University, Beijing, 100044, China.

<sup>‡</sup> These authors contributed equally.

E-mail: qhcui@bjtu.edu.cn; qunxu@zzu.edu.cn; weicong@zzu.edu.cn.

## **Materials and methods**

### **Materials**

CdCl<sub>2</sub>, ZnCl<sub>2</sub>, SnCl<sub>2</sub>, LiCl, citric acid, tetrabutyl titanate, thiourea and ammonium molybdate tetrahydrate were obtained from Shanghai Aladdin Biochemical Technology Co., Ltd. The soluble starch was provided by Sinopharm Chemical Reagent Co., Ltd (China). Glycerol, acetic acid, oleic acid and triton X-100 were purchased from J&K Scientific Ltd. (Beijing, China). All the chemicals were used without further treatment.

### **Synthesis procedure of 2D CdS film**

2D CdS film was synthesized via a gas-liquid heterogeneous reaction. Typically, 50 mg CdCl<sub>2</sub> and a certain amount of starch were successively added into 10 g glycerol under magnetic stirring for 30 min at 120 °C. The viscosity of mixed solution can be significantly regulated by adjusting the amount of the added soluble starch. 200 μL CdCl<sub>2</sub>/starch/glycerin solution was extracted and dropped onto an ultra-clean glass substrate, and positioned 15 cm downstream away from the center zone of the tube furnace as the liquid Cd precursor. 100 mg thiourea powders were placed at the center of the tube furnace to produce gaseous sulfur precursor. The tube was sealed and purged with N<sub>2</sub> for 20 minutes. Then the temperature of the center zone was heated to 180 °C in 20 min and maintained at this set temperature for 120 min under a constant N<sub>2</sub> flow of 100 standard cubic centimeter per minute. After the reaction, the furnace was cooled to room temperature naturally. The obtained CdS film was floating on the liquid surface and was washed alternately with hot glycerol and dimethylformamide (DMF) for five cycles. The floating CdS film was then fished out of the DMF to any desired substrate (TEM grid, glass, PET or SiO<sub>2</sub>) and dried in an oven at 80 °C for subsequent characterization and device fabrication.

### **Synthesis procedure of 2D ZnS film**

2D ZnS film was synthesized via a similar method. In a routine process, 3 g starch and 30 mg ZnCl<sub>2</sub> and 50 mg citric acid were added in turn to 10 g glycerin and well mixed under magnetic stirring for 30 min at 120 °C. 200 μL ZnCl<sub>2</sub>/starch/ citric acid /glycerin mixed solution was extracted and dropped onto an ultraclean glass substrate, and positioned 15 cm downstream away from the center zone of the tube furnace

as the liquid Zn precursor. In order to prepare gaseous sulfur precursor, 100 mg thiourea powders were placed at the center of tube furnace. The tube was sealed and purged with N<sub>2</sub> for 20 minutes. Then the temperature of the center zone was heated to 160 °C in 20 min and maintained at this set temperature for 120 min under a constant N<sub>2</sub> flow of 100 standard cubic centimeter per minute. After finishing the reaction, the obtained ZnS film was washed alternately with hot glycerol and DMF for five cycles. Then, the floating ZnS film was fished out of the DMF to any desired substrate (TEM grid, glass, PET or SiO<sub>2</sub>) and dried in an oven at 80 °C for subsequent characterization.

### **Synthesis procedure of 2D TiO<sub>2</sub> film**

Typically, 50 μL tetrabutyl titanate, 50 μL acetic acid, 500 μL oleic acid and 4.5 mL triton X-100 were evenly mixed under magnetic stirring for 30 min. The reaction process was performed in a horizontal tubular furnace. 200 μL mixed solution was extracted and dropped onto an ultraclean glass substrate, and positioned downstream away from the center zone of the tube furnace. 10 ml of deionized water put in an aluminium oxide boat was placed at the center of tube furnace. Subsequently, the temperature of the center zone was heated to 90 °C in 20 min and maintained at this set temperature for 60 min under the atmosphere. Centimeter-scale high-quality TiO<sub>2</sub> film obtained was washed with deionized water for three times. Then, the floating TiO<sub>2</sub> film was fished out of the deionized water to any desired substrate (TEM grid, glass, PET or SiO<sub>2</sub>) and dried in an oven at 80 °C for subsequent characterization.

### **Synthesis procedure of 2D SnO<sub>2</sub> film**

3 g starch and 30 mg SnCl<sub>2</sub> and 800 mg LiCl were added to 10 g glycerin and well mixed under magnetic stirring for 30 min at 120 °C. 200 μL mixed solution was extracted and dropped onto an ultraclean glass substrate, and positioned downstream away from the center zone of the tube furnace. 15 ml of deionized water put in an aluminium oxide boat was placed at the center of tube furnace. Then the temperature of the center zone was heated to 170 °C in 20 min and maintained at this set temperature for 60 min under the atmosphere. Finally, in order to remove excess inorganic salts and organics, the obtained SnO<sub>2</sub> film was washed alternately with deionized water and DMF for several times. Then, the floating SnO<sub>2</sub> film was

fished out of the DMF to any desired substrate (TEM grid, glass, PET or SiO<sub>2</sub>) and dried in an oven at 80 °C for subsequent characterization.

### **Synthesis procedure of 2D MoS<sub>2</sub> film**

3 g starch and 50 mg (NH<sub>4</sub>)<sub>6</sub>Mo<sub>7</sub>O<sub>24</sub>·4H<sub>2</sub>O were added into 10 g glycerol and well mixed under magnetic stirring for 30 min at 120 °C. 200 μL mixed solution was extracted and dropped onto an ultraclean glass substrate, and positioned 5 cm downstream away from the center of the tube furnace as the liquid Mo sources. 100 mg thiourea powders were placed at the center zone to produce gaseous sulfur precursor. The tube was sealed and purged with N<sub>2</sub> for 20 minutes. Then the temperature of the center zone was heated to 190 °C in 20 min and maintained at this set temperature for 120 min under a constant N<sub>2</sub> flow of 100 standard cubic centimeter per minute. The obtained MoS<sub>2</sub> film was washed alternately with hot glycerol and DMF for five cycles. The floating film was then fished out of the DMF to any desired substrate (TEM grid, glass, PET or SiO<sub>2</sub>) and dried in an oven at 80 °C for subsequent characterization.

### **Devices Fabrication and Performance**

The mask template (copper mesh) was fixed onto the clean CdS film using high-temperature resistant tape, and then transferred to a vacuum thermal evaporation system (Nexdep, Angstrom Engineering) for Au electrode deposition. Au electrodes (70 nm thickness) with a channel width of 25 μm were deposited on CdS film to construct the planar photodetectors. The effective area of each device was 1.45×10<sup>-5</sup> cm<sup>2</sup>. The photoresponse characteristics were measured using a probe station and the Keithley 4200 semiconductor characterization system under various bias voltages and power densities.

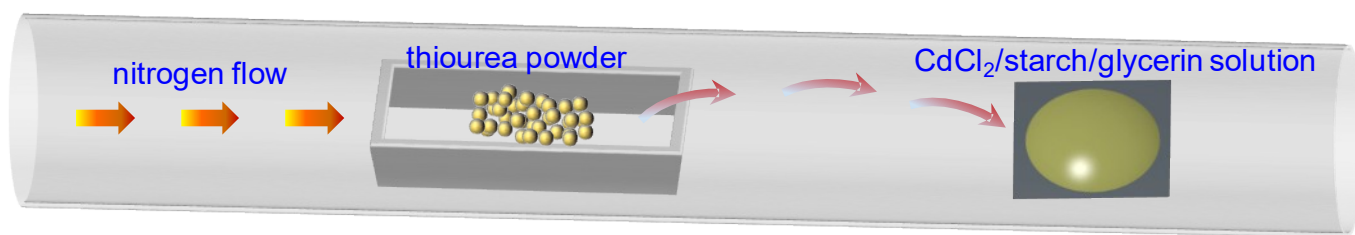


**Figure S1. Scheme of the gas-liquid reaction set-up for the growth of CdS film.**

As shown in Figure S1, an aluminium oxide boat containing thiourea powder was placed in the center of the tube, while CdCl<sub>2</sub>/starch/glycerin solution was placed on the down-stream of the tube furnace as the liquid precursor. Under thermal treatment, gaseous thiourea molecules would diffuse and encounter with the liquid Cd precursor at the interface, forming a typical gas-liquid reaction.

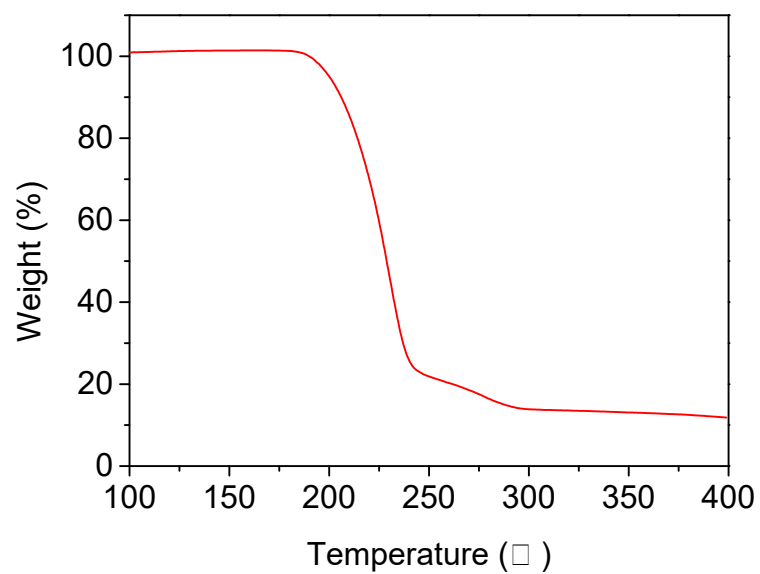


**Figure S2. TG curve of the thiourea molecules.**

As shown in Figure S2, thiourea began to lose weight above 175 °C in the nitrogen atmosphere, indicating that thiourea molecules would undergo significant gasification and pyrolysis when the temperature exceeds 175 °C.<sup>1</sup>

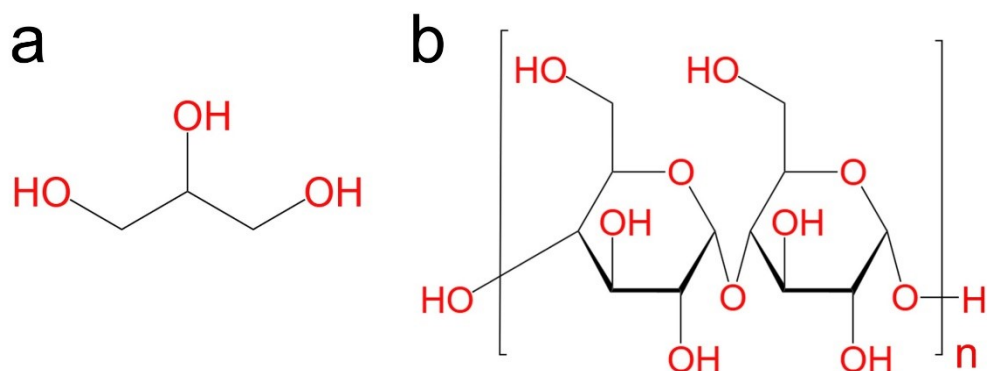


**Figure S3. The chemical structural of glycerol (a) and starch (b) molecules.**

As shown in Figure S3a, the glycerol molecule contained three hydroxyl groups (-OH), and the oxygen atom in each hydroxyl group (with high electronegativity) can form a strong hydrogen bond with the hydroxyl groups of adjacent molecules. The hydroxyl groups of glycerol were spatially flexibly distributed, which could form a multi-dimensional hydrogen bond network, greatly increasing the binding energy between liquid molecules. Higher energy was required to disrupt these effects, resulting in a boiling point reaching 290 °C.<sup>2</sup> High boiling point glycerol provided a stable interface for the anisotropic growth of 2D centimeter-scale films.

In addition, starch gelatinization occurs at high temperature, and the gelatinized starch chains entangle with each other. Moreover, a large number of hydroxyl groups (-OH) in starch molecules formed hydrogen bond interaction with glycerol molecules (Figure S3b), which increased the viscosity of the system. The viscosity of the system was controlled by adjusting the addition amount of starch to manipulate the diffusion rate of  $\text{Cd}^{2+}$ , achieving low vertical reaction rate.

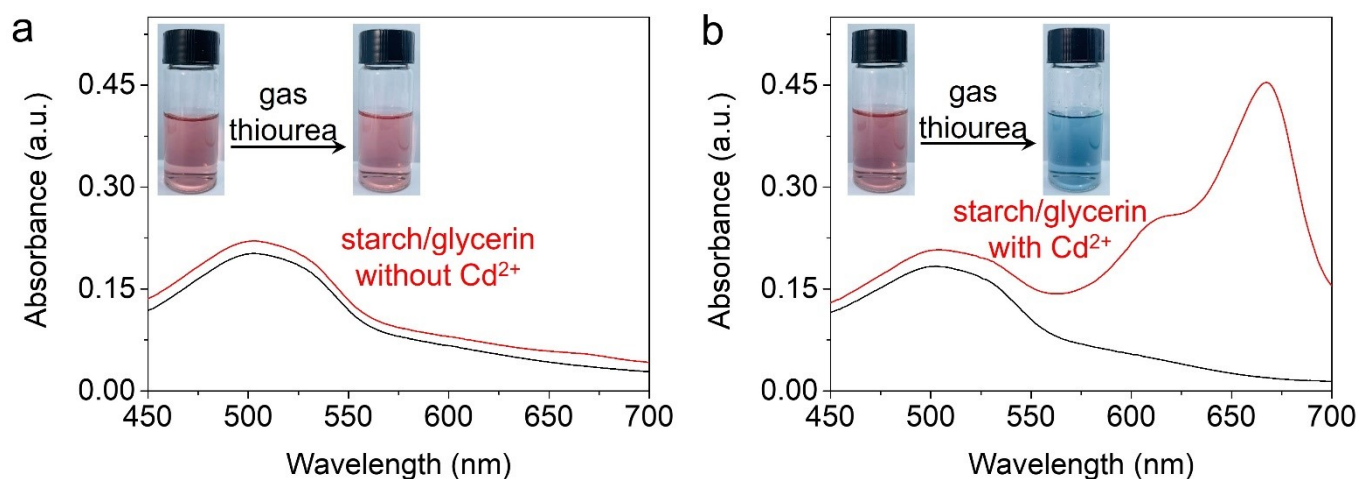


**Figure S4. Detection of the sulfides in the starch/glycerin solution via the methylene blue spectrophotometric assay.** (a) UV-vis absorption spectra of the reagents (N,N-dimethyl-p-phenylenediamine and ammonium iron sulfate) pretreated starch/glycerin solution without CdCl<sub>2</sub> before (black) and after (red) the treatment of the thiourea steam. (b) UV-vis absorption spectra of the reagents (N,N-dimethyl-p-phenylenediamine and ammonium iron sulfate) pretreated CdCl<sub>2</sub>/starch/glycerin solution before (black) and after (red) the treatment of the thiourea steam. Insets are the corresponding photographs.

The methylene blue spectrophotometric assay is based on the reaction of sulfide, ammonium iron (III) sulfate, and N, N-dimethyl-p-phenylenediamine to produce methylene blue, which is widely used for the determination of trace sulfides.<sup>3,4</sup> In our procedure, 0.5 ml sample was first diluted with 20 ml of water and then mixed with the reagents in a sealed vial. The reagents used in our work include 6 mol L<sup>-1</sup> hydrochloric acid (1 ml), 2 g L<sup>-1</sup> N, N-dimethyl-p-phenylenediamine solution (1 ml) and 100 g L<sup>-1</sup> ammonium iron (II) sulfate (0.1 mL). The absorbance of methylene blue was measured using the Lambda 1050 Perkin-Elmer spectrophotometer.

As shown in Figure S4a, for liquid precursor without CdCl<sub>2</sub>, the color of the pretreated solution did not change significantly before and after the treatment of the thiourea steam. No characteristic absorption peaks of methylene blue appeared in the corresponding absorption spectra, indicating that the condensation transition of the gaseous sulfur was severely suppressed in this situation. While, when the CdCl<sub>2</sub> was

involved, the color of the pretreated solution changed from pink to blue after the treatment of thiourea steam. Two new peaks at 610 and 664 nm were observed in the corresponding UV-vis spectrum, which is well consistent with the characteristic peaks of methylene blue (Figure S4b). This provided an compelling evidence for the successful capture of gaseous sulfur in the presence of cadmium ions, further confirming our hypothesis of the gas-liquid non-homogeneous reactions in the main text.

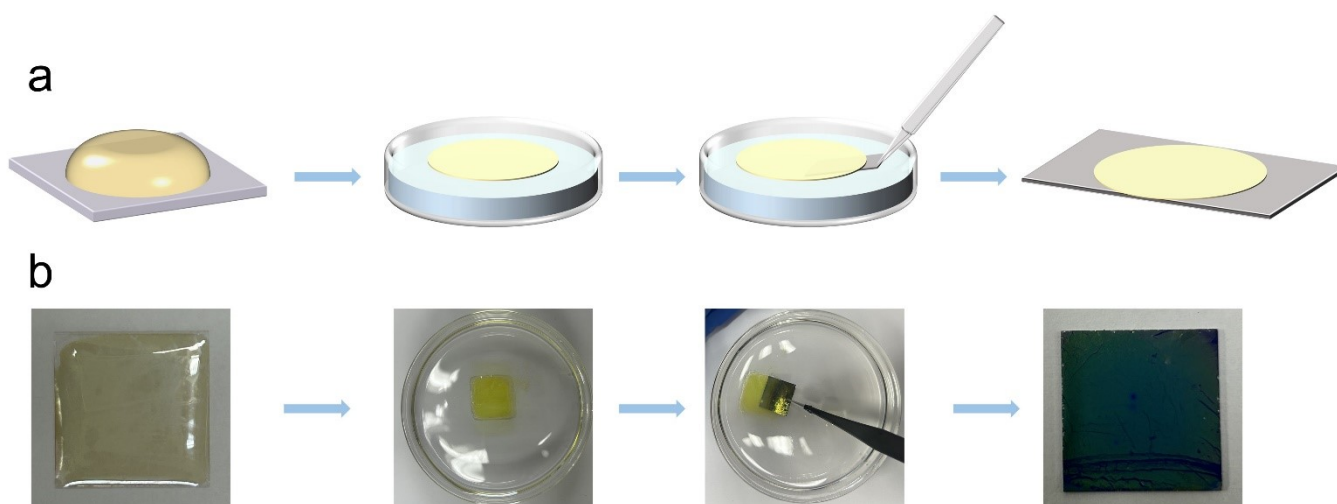


**Figure S5. Transfer process of the as-grown CdS film.** Scheme (a) and photograph (b) of CdS film transfer onto SiO<sub>2</sub> substrate.

As shown in Figure S5, the CdS film naturally floated on the surface of the liquid phase (CdCl<sub>2</sub>/starch/glycerin solution). The light yellow CdS film exhibited smooth morphology and centimeter-scale lateral dimensions. The glass sheet carrying the CdS film was slowly immersed into a dimethylformamide (DMF) bath. The CdS film naturally separated from the glass sheet and floated on the surface of DMF solution. The solvent was exchanged with fresh DMF for many times to remove residual starch, glycerol and unreacted precursors. Then, a clean substrate was slowly immersed under the CdS film at a controlled angle ( $\sim 30^\circ$ - $45^\circ$ ), to minimized the disturbance of DMF solution. This step ensured uniform contact between the substrate and the floating film. Gently lifted the SiO<sub>2</sub> substrate with CdS film from the liquid with tweezers, so that the CdS film could be attached to the substrate. Then, the transferred film was placed in a vacuum oven at 80°C for 60 minutes to evaporate the residual solvent (DMF), which eliminated interfacial bubbles and enhanced the adhesion between the film and the substrate. This method retains the structural integrity and cleanliness of 2D CdS films, which is of profound significance for subsequent characterization, integration and deviceization.

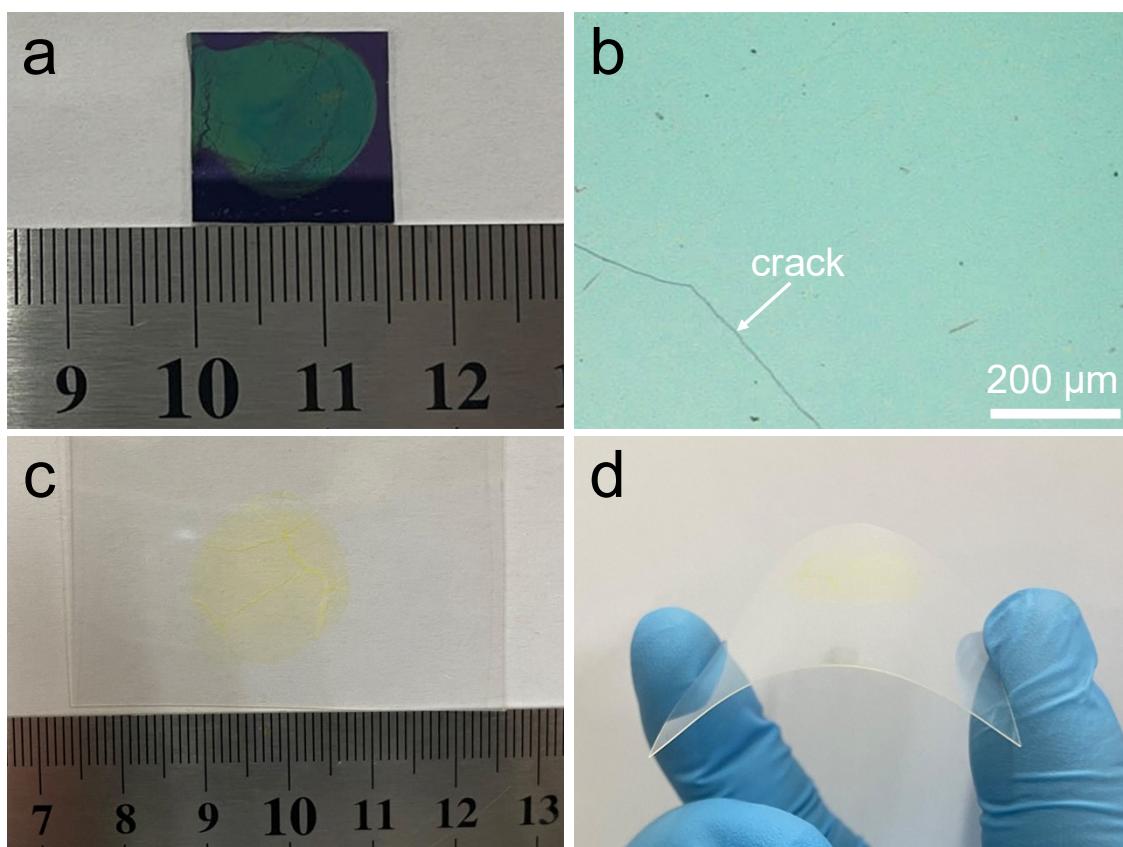


**Figure S6. Optical images of the CdS films transferred to different substrates.** Photograph (a) and optical microscopy image (b) of the 2D CdS film transferred onto the SiO<sub>2</sub>/Si substrate. (c, d) Photographs of the 2D CdS film transferred onto the flexible PET substrate.

2D CdS film was formed at the gas-liquid interface and was eventually floating on the liquid surface, enabling effortless transfer of the 2D film to various substrates. As depicted in Figure S6a-b, the CdS thin film was successfully transferred to the SiO<sub>2</sub>/Si substrate, facilitating the subsequent construction of the optoelectronic devices.<sup>5</sup> Furthermore, CdS thin film can also be composited with the flexible PET substrate and bent along with it without peeling, demonstrating its excellent mechanical flexibility (Figure S6c-d).<sup>6</sup>

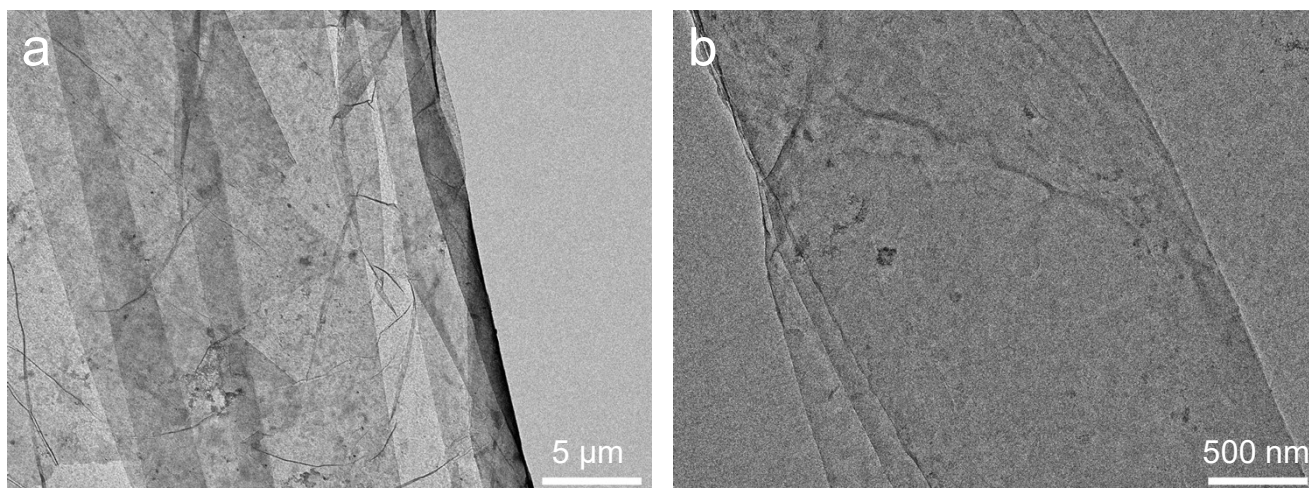


**Figure S7. (a, b) Low-magnification TEM images of the 2D CdS film.**

As shown in Figure S7, the as-prepared 2D CdS film is nearly transparent and has a low contrast with the background, demonstrating its ultra-thin nature.

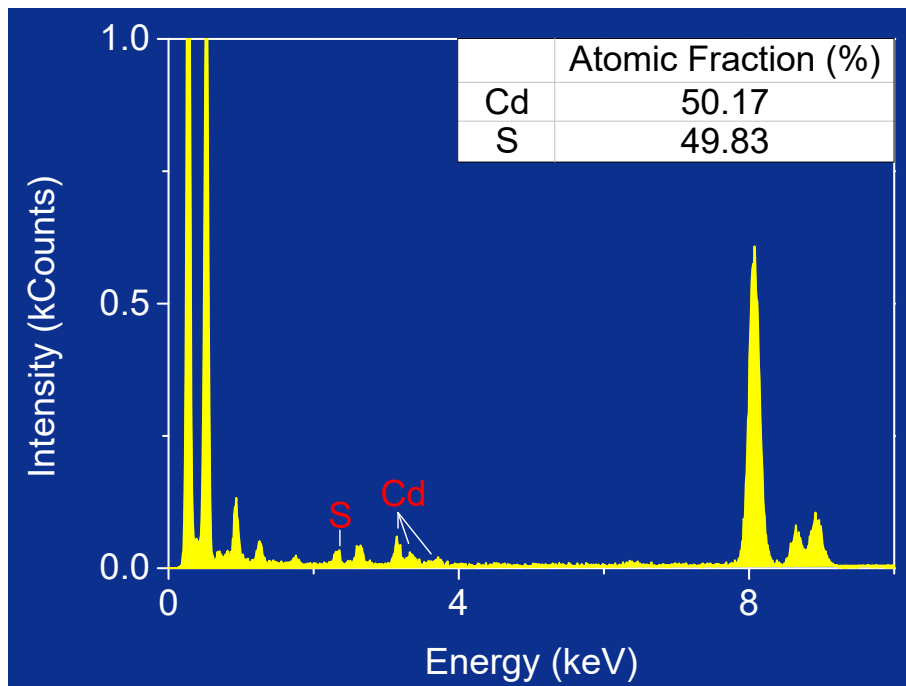


**Figure S8. EDS spectrum of the 2D CdS film.**

As shown in Figure S8, the Cd/S molar ratio was 50.17:49.83, which is in agreement with the stoichiometric ratio (1:1) of the CdS crystal.

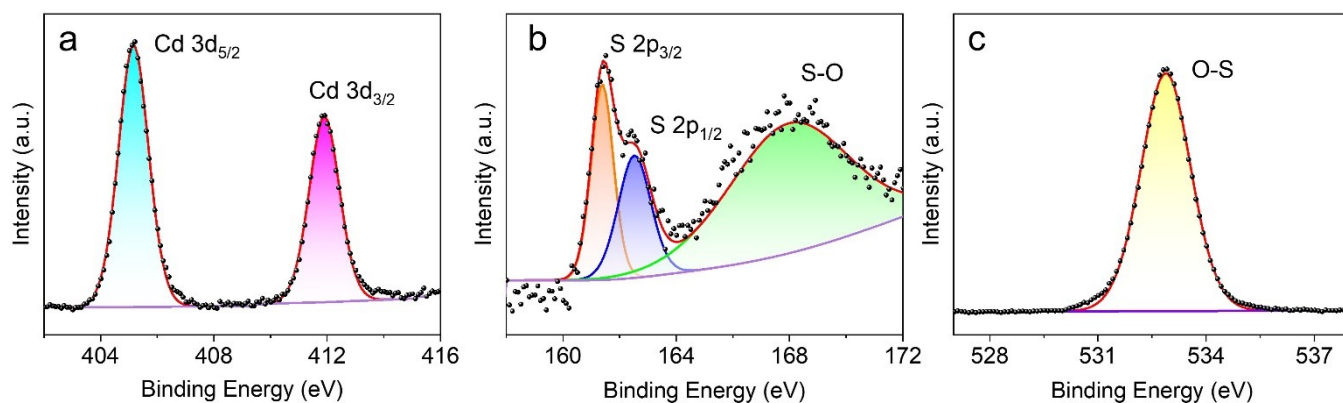


**Figure S9. Bottom surface chemical states of the ultrathin 2D-CdS. XPS spectra of Cd 3d (a) and S 2p (b) and O 1s (c) for the 2D CdS film.**

As shown in Figure S9, the bottom surface (direct contact with the glycerol/starch liquid precursors) chemical states and compositions of 2D-CdS film were characterized by XPS. From the investigation spectrum of Cd 3d, the peaks of Cd 3d<sub>5/2</sub> (405.2 eV) and Cd 3d<sub>3/2</sub> (411.8 eV) could be clearly identified, which correspond to Cd<sup>2+</sup> (Figure S9a). The diffraction peaks of S 2p of CdS could be well fitted at 161.5 eV and 162.7 eV, corresponding to the S 2P<sub>3/2</sub> and S 2P<sub>1/2</sub> orbitals respectively, which attributed to S<sup>2-</sup>. Another peak at 167.8 eV could be attributed to S-O bonds, well consistent with the top surface chemical states (Figure S9b). However, the bottom surface of the CdS film was in close contact with the liquid phase, and there was a large amount of hydroxyl in glycerol and starch, resulting in a higher overall content of S-O on the bottom surface film than on the top surface of the 2D CdS film (Figure 3e). The high-resolution O 1s spectrum fitted a peak at 532.8 eV, which was consistent with the O-S bond (Figure S9c).

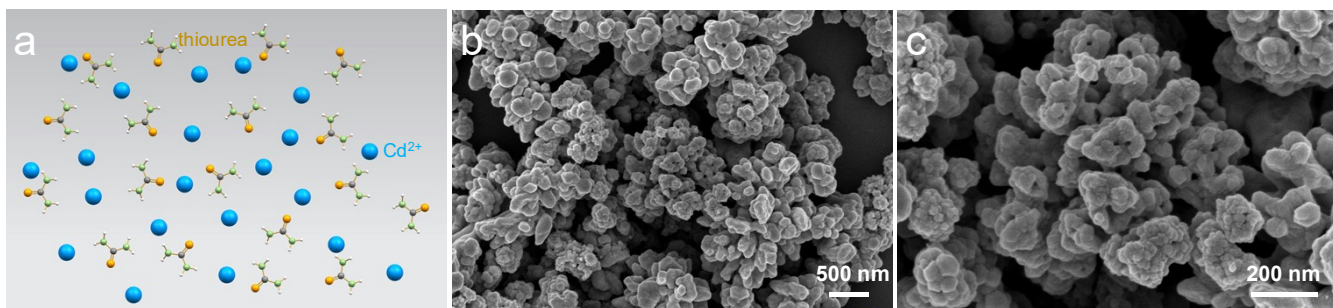


**Figure S10. Homogeneous synthesis of CdS particles.** (a) Schematic illustration of the homogeneous synthesis of CdS. (b, c) SEM images of CdS crystals obtained via a homogeneous reaction.

A homogeneous reaction system was carried out as a control experiment, Cd and S precursors are well mixed in starch/glycerin solution and can migrate freely (Figure S10a). The morphology of the product is mainly determined by the surface lattice energy.<sup>7</sup> As shown in Figure S10b-c, only nanoparticles rather than 2D shaped crystals were obtained, conforming the gas-liquid heterogeneous reaction system was the key point for the formation of the 2D CdS film.

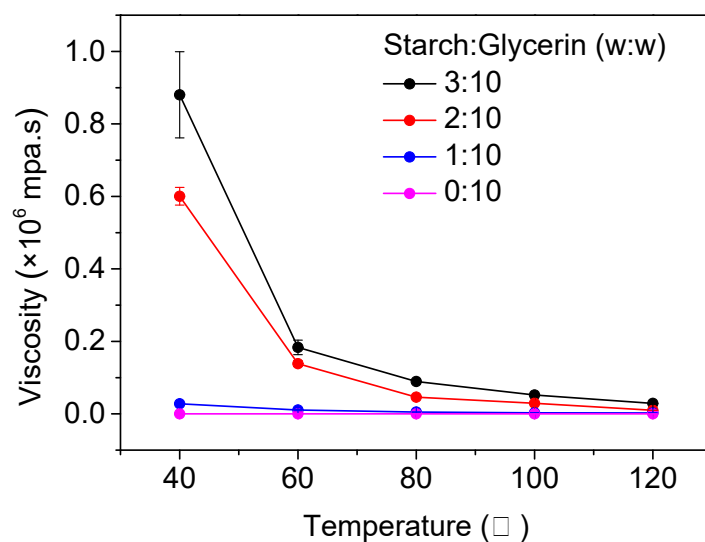


**Figure S11. Viscosity curves of the starch/glycerin solution versus temperature.**

As shown in Figure S11, the viscosity of the starch/glycerin increases with increasing the starch content and decreases significantly with increasing the temperature, enabling us to effectively regulate the diffusion coefficient of precursor in liquid phase by changing the viscosity of the starch/glycerin solution.

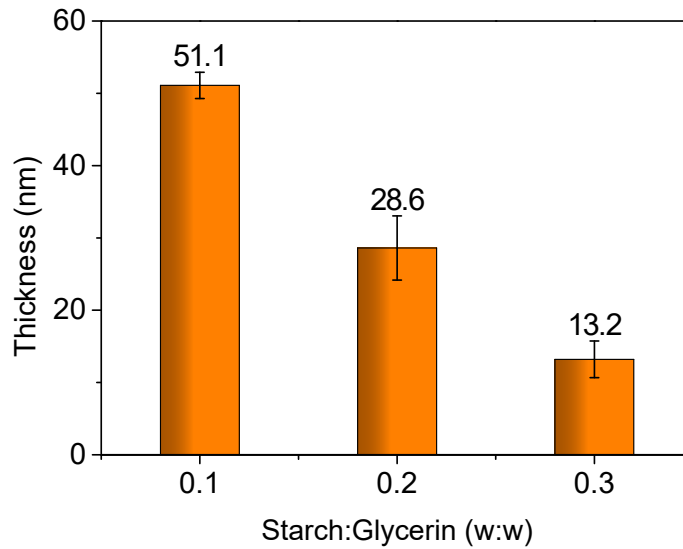


**Figure S12. Average thicknesses of the obtained CdS films versus the starch/glycerol ratio.**

We randomly selected 15 CdS films that obtained at different starch/glycerol ratios (select 5 for each condition) and analyzed them with AFM to obtain their average thicknesses. As shown in Figure S12, the average thicknesses of the obtained CdS films are about 51, 28 and 13 nm when the starch/glycerin weight ratio is 0.1, 0.2 and 0.3, respectively.

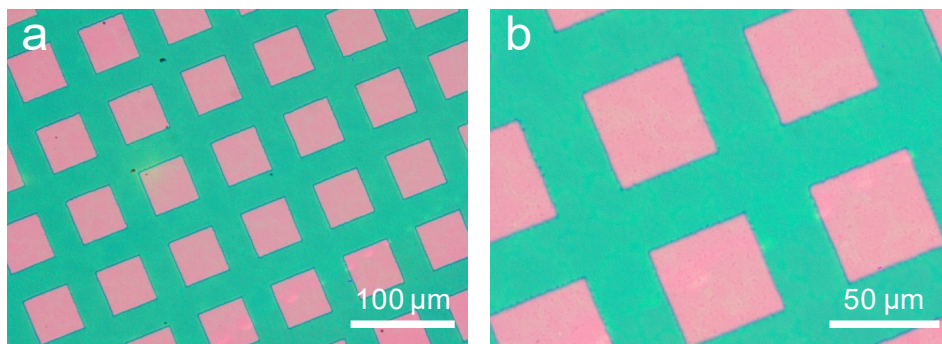


**Figure S13. (a, b) Optical microscopy image of Au electrode arrays deposited on the 2D CdS film.**

Our photodetector device was fabricated by thermally depositing Au electrodes on the CdS film using a copper mesh as the mask. As shown in Figure S13, hundreds of electrodes can be simultaneously deposited on the centimeter-scale of the CdS film, making it possible for the subsequent integration of large-scale device arrays.

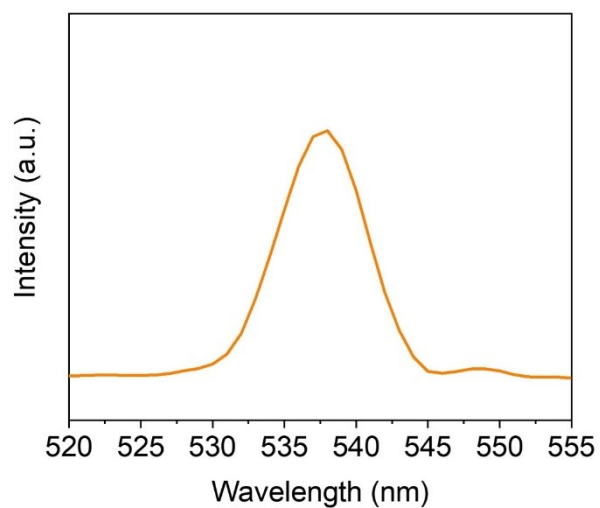


**Figure S14. PL spectra of CdS film.**

As shown in Figure S14, the 2D CdS film exhibited a photoluminescence emission peak centered at 538 nm under excitation at 360 nm, aligning with the band gap value obtained from UV-vis absorption spectra (Figure 6b,  $\sim 2.49$  eV).<sup>8</sup>

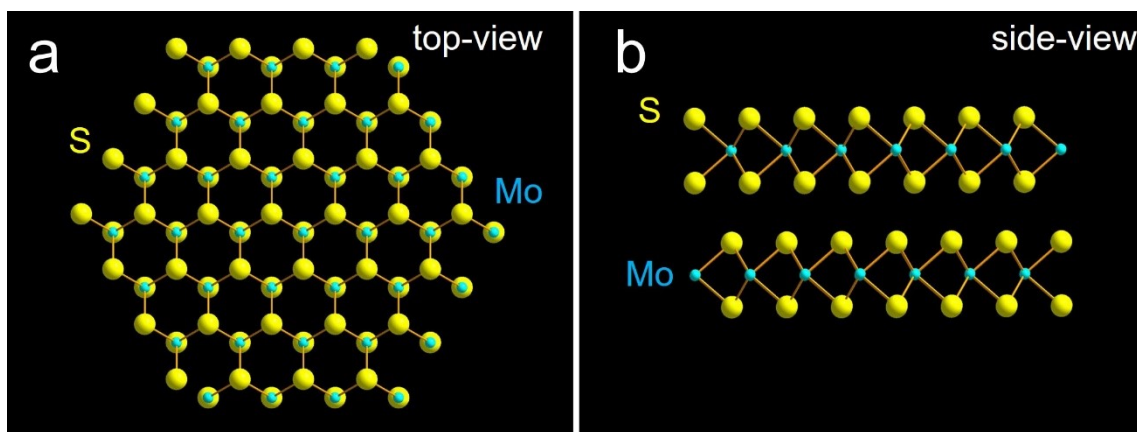


**Figure S15. Structure of MoS<sub>2</sub>. Top view (a) and side view (b) of the bilayer MoS<sub>2</sub>.**

As shown in Figure S15, layered MoS<sub>2</sub> exhibits a trilayer configuration structure in the form of S-Mo-S. This configuration features two layers of S atoms arranged in a 2D hexagonal lattice stacked together, with Mo atoms positioned at the center of triangular prismatic cages formed by six S atoms. The Mo and S atoms are interconnected via covalent bonds within the layers, while adjacent MoS<sub>2</sub> layers are held together by van der Waals interactions.

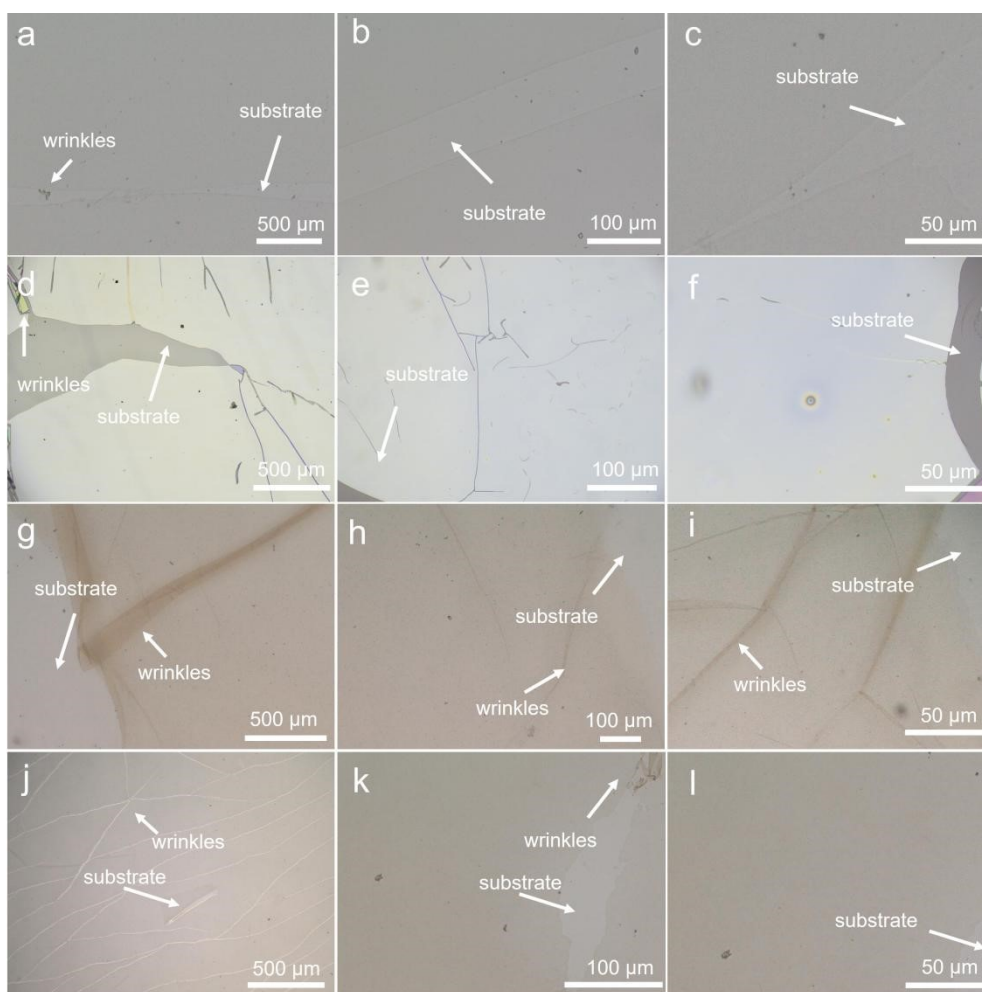


**Figure S16. Photographs of ZnS, TiO<sub>2</sub>, SnO<sub>2</sub> and MoS<sub>2</sub> films.** Optical images of the ZnS (a, b, c), TiO<sub>2</sub> (d, e, f), SnO<sub>2</sub> (g, h, i) and MoS<sub>2</sub> (j, k, l) films transferred onto the glass substrates.

As shown in Figure S16, the obtained semiconductor films showed homogeneous appearance under optical imaging, indicating the uniform thickness of the synthesized films.

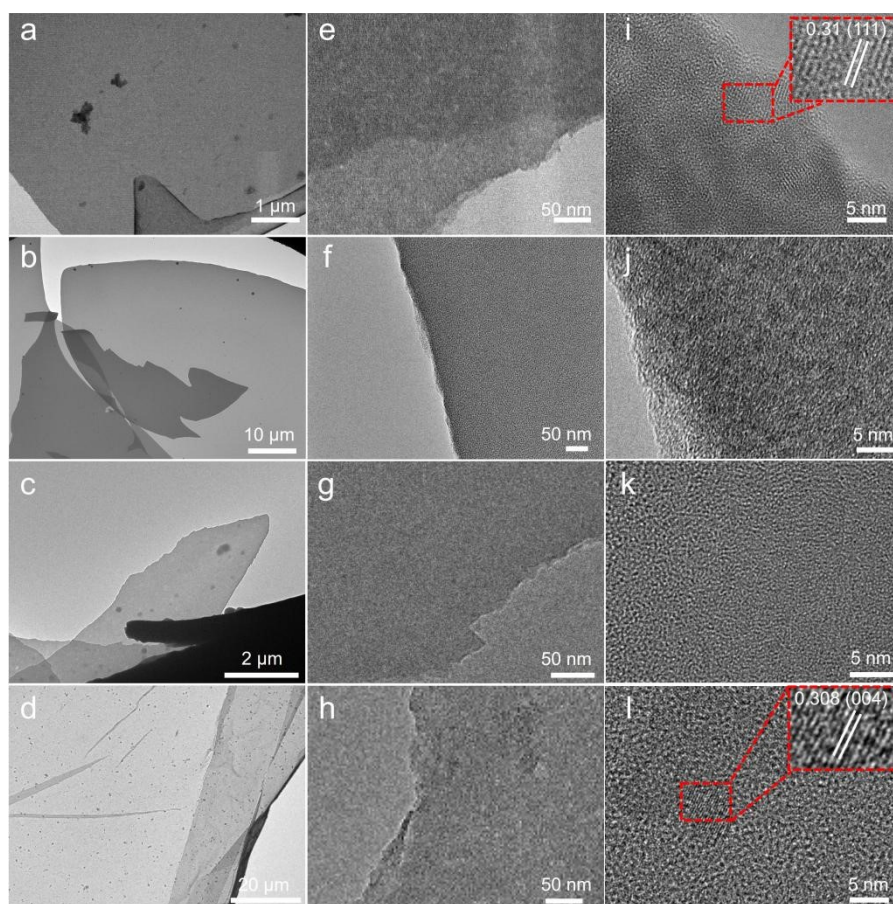


**Figure S17. Morphology and structure characterizations of ZnS, TiO<sub>2</sub>, SnO<sub>2</sub> and MoS<sub>2</sub> films.** Low-magnification TEM images of the ZnS (a, e), TiO<sub>2</sub> (b, f), SnO<sub>2</sub> (c, g) and MoS<sub>2</sub> (d, h) films. HRTEM images of the ZnS (i), TiO<sub>2</sub> (j), SnO<sub>2</sub> (k) and MoS<sub>2</sub> (l) films.

As shown in Figure S17a-h, the typical TEM images of the obtained 2D semiconductor materials showed film-like structures with a high degree of transparency, indicating that free-standing 2D films with ultrathin nature were obtained.<sup>9</sup> The HRTEM results revealed that the TiO<sub>2</sub> (Figure S17j) and SnO<sub>2</sub> (Figure S17k) were amorphous. While, the ZnS (Figure S17i) and MoS<sub>2</sub> (Figure S17l) films were mainly amorphous with only a few nano-scale crystalline regions. The HRTEM images corroborated that lattice spacing of the lattice fringes were 0.31 nm and 0.308 nm, which were in good agreement with the (111) and (004) planes of the ZnS and MoS<sub>2</sub> crystal structures, respectively.

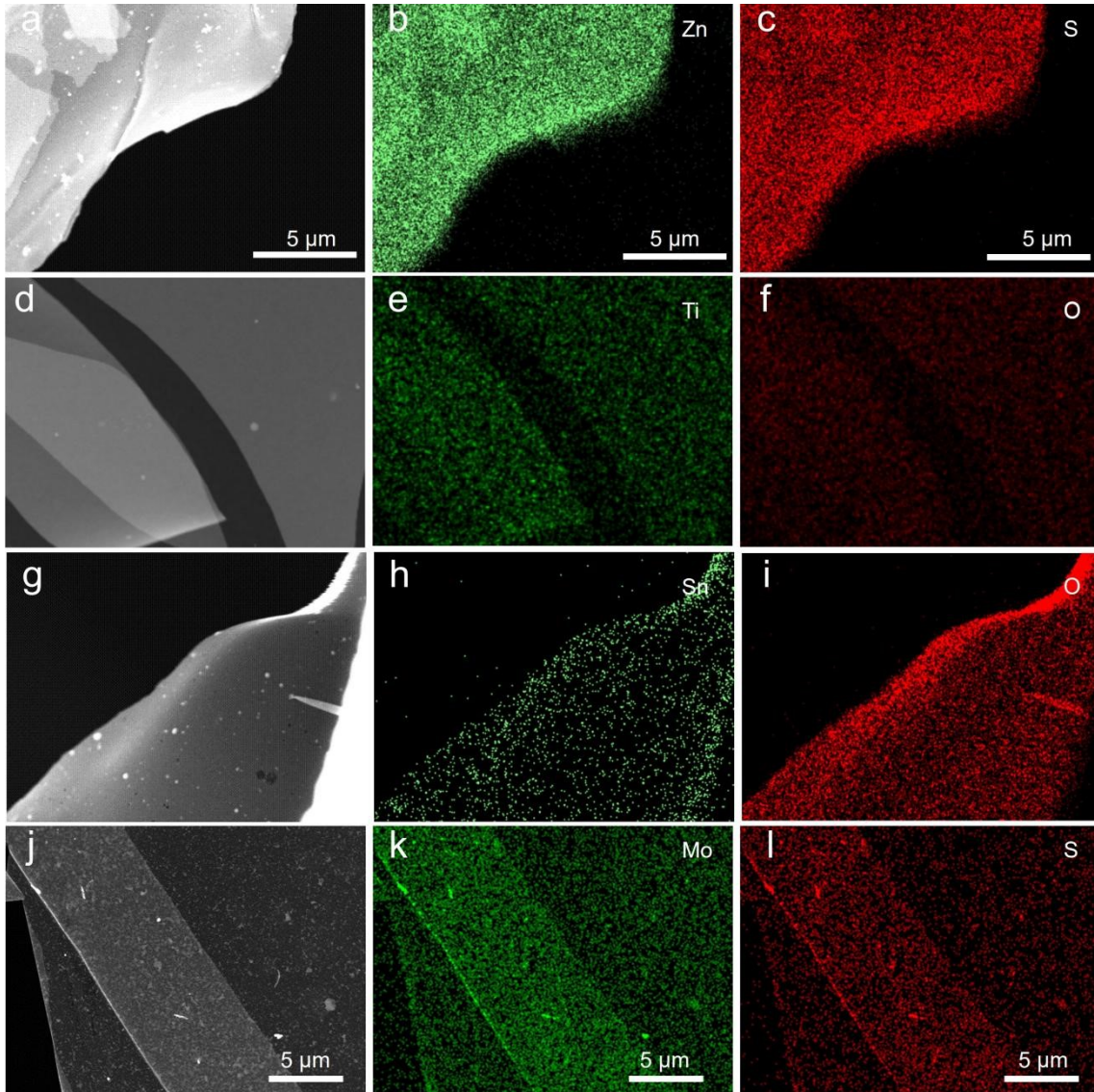


**Figure S18. Composition characterizations of ZnS, TiO<sub>2</sub>, SnO<sub>2</sub> and MoS<sub>2</sub> films.** STEM image of the synthesized ZnS (a), TiO<sub>2</sub> (d), SnO<sub>2</sub> (g) and MoS<sub>2</sub> (j) film. EDS analysis mapping of Zn (b) and S (c) of the ZnS film, Ti (e) and O (f) of the TiO<sub>2</sub> film, Sn (h) and O (i) of the SnO<sub>2</sub> film, and Mo (k) and S (l) of the MoS<sub>2</sub> film.

As shown in Figure S18, the involved elements were homogeneous distributed over the 2D centimeter-scale semiconductor films.

## References:

1. Z. D. Wang, M. Yoshida and B. George, Theoretical study on the thermal decomposition of thiourea, *Comput Theor Chem*, 2013, **1017**, 91-98.
2. N. Yadav, G. Yadav and M. Ahmaruzzaman, Catalytic conversion and mechanism of glycerol into various value-added products: a critical review, *Ind. Crops Prod.*, 2024, **210**, 117999.
3. H. M. Smith and M. D. Pluth, Advances and opportunities in H<sub>2</sub>S measurement in chemical biology, *JACS Au*, 2023, **3**, 2677-2691.
4. J. K. Fogo and M. Popowsky, Conversion of sulfur compounds to hydrogen sulfide in air, fuel gas, or mixtures, *Anal. Chem.*, 1949, **21**, 734-737.
5. H.-k. Jo, J. Kim, Y. R. Lim, S. Shin, D. S. Song, G. Bae, Y. M. Kwon, M. Jang, S. Yim, S. Myung, S. S. Lee, C. G. Kim, K. K. Kim, J. Lim and W. Song, Wafer-Scale Production of Two-Dimensional Tin Monoselenide: Expandable Synthetic Platform for van der Waals Semiconductor-Based Broadband Photodetectors, *ACS Nano*, 2023, **17**, 1372-1380.
6. A. K. Katiyar, A. T. Hoang, D. Xu, J. Hong, B. J. Kim, S. Ji and J.-H. Ahn, 2D Materials in Flexible Electronics: Recent Advances and Future Prospectives, *Chem. Rev.*, 2024, **124**, 318-419.
7. C. Sun, S. Mao, D. Yu, M. Xue and X. Sun, Synthesis, characterization, and photocatalytic application of cadmium(II) sulfide-magnetite in one-pot multi-component synthesis of some 1-amidoalkyl-2-naphthols, *J. Mol. Struct.*, 2024, **1312**, 138451.
8. C. Qin, Y. Gao, Z. Qiao, L. Xiao and S. Jia, Atomic-layered MoS<sub>2</sub> as a tunable optical platform, *Adv. Opt. Mater.*, 2016, **4**, 1429-1456.
9. A. Zavabeti, J. Z. Ou, B. J. Carey, N. Syed, R. Orrell-Trigg, E. L. H. Mayes, C. Xu, O. Kavehei, A. P. O'Mullane, R. B. Kaner, K. Kalantar-zadeh and T. Daeneke, A liquid metal reaction environment for the room-temperature synthesis of atomically thin metal oxides, *Science*, 2017, **358**, 332-335.